

UCRL- 84040  
PREPRINT

MECHANICAL PROPERTIES OF HIGH-CURRENT MULTIFILAMENTARY

$\text{Nb}_3\text{Sn}$  CONDUCTORS

R. M. Scanlan, R. W. Hoard, D. N. Cornish,  
and J. P. Zbasnik

This paper was prepared for submittal to  
International Cryogenic Materials Conference  
Upton, New York  
May 28-29, 1980

May 23, 1980



Lawrence  
Livermore  
Laboratory

This is a preprint of a paper intended for publication in a journal or proceedings. Since changes may be made before publication, this preprint is made available with the understanding that it will not be cited or reproduced without the permission of the author.

CIRCULATION COPY  
SUBJECT TO RECALL  
IN TWO WEEKS

#### DISCLAIMER

This document was prepared as an account of work sponsored by an agency of the United States Government. Neither the United States Government nor the University of California nor any of their employees, makes any warranty, express or implied, or assumes any legal liability or responsibility for the accuracy, completeness, or usefulness of any information, apparatus, product, or process disclosed, or represents that its use would not infringe privately owned rights. Reference herein to any specific commercial product, process, or service by trade name, trademark, manufacturer, or otherwise, does not necessarily constitute or imply its endorsement, recommendation, or favoring by the United States Government or the University of California. The views and opinions of authors expressed herein do not necessarily state or reflect those of the United States Government or the University of California, and shall not be used for advertising or product endorsement purposes.

# MECHANICAL PROPERTIES OF HIGH-CURRENT MULTIFILAMENTARY Nb<sub>3</sub>Sn CONDUCTORS\*

R. M. Scanlan, R. W. Hoard, D. N. Cornish, and  
J. P. Zbasnik

University of California  
Lawrence Livermore National Laboratory

Livermore, CA 94550

## INTRODUCTION

Nb<sub>3</sub>Sn is a strain-sensitive superconductor which exhibits large changes in properties for strains of less than 1 percent. The critical current density at 12 T undergoes a reversible degradation of a factor of two for compressive strains of about 1 percent and undergoes an irreversible degradation for tensile strains on the Nb<sub>3</sub>Sn greater than 0.2 percent. Consequently, the successful application of Nb<sub>3</sub>Sn in large high-field magnets requires a complete understanding of the mechanical properties of the conductor. One conductor which is being used for many applications<sup>1-3</sup> consists of filaments of Nb<sub>3</sub>Sn in a bronze matrix, and much progress has been made in understanding the mechanical behavior of this composite.<sup>4</sup> The Nb<sub>3</sub>Sn filaments are placed in compression due to the differential thermal contraction between Nb<sub>3</sub>Sn and bronze which occurs when the composite is cooled from the Nb<sub>3</sub>Sn formation temperature (typically 700 °C) to the 4.2 K operating temperature. The general behavior of the critical current when this conductor is subjected to a tensile stress is an increase to a maximum when the compressive strain on the Nb<sub>3</sub>Sn is relieved, followed by a decrease as the Nb<sub>3</sub>Sn filaments are placed in tension. The degree of precompression is controlled largely by the ratio of bronze to Nb<sub>3</sub>Sn in the conductor.<sup>5</sup>

---

\*Work performed under the auspices of the U.S. Department of Energy by the Lawrence Livermore National Laboratory under Contract W-7405-Eng-48.

Several authors<sup>6,7</sup> have presented analytical methods which can be used to estimate the residual strain on the Nb<sub>3</sub>Sn and hence to predict the strain-critical current behavior of the conductor. These methods have been shown to work well for a specific type of conductor, i.e., Nb<sub>3</sub>Sn filaments in a bronze matrix. However, these methods are not adequate to explain the results when other conductor geometries are used or when additional compressive strain occurs due to other components in the conductor. In this paper, we present results for a composite geometry in which the triaxial strain state is important, and we present a computer code which can predict the conductor behavior (as well as the behavior of the bronze-matrix-type conductor). In addition, we present results for several practical conductors in which precompression due to components other than the bronze matrix is important.

#### BRONZE CORE, Nb TUBE CONDUCTOR

After the discovery that Nb<sub>3</sub>Sn could be fabricated by reacting Nb with Sn provided by a bronze matrix, a number of different multifilamentary configurations were proposed. One configuration, which we designate as the internal bronze approach, consists of Nb tubes with bronze cores in a copper matrix. This configuration has several potential advantages over the external bronze approach, namely the Nb tubes serve as diffusion barriers so that another element such as Ta is not necessary to prevent Sn from contaminating the Cu, and each superconductor element is surrounded by a high conductivity Cu matrix so that current transfer lengths are much shorter than in the external bronze case.

The fabrication and testing of several conductors based on this approach are described in Ref. 8. A computer program was developed which evaluates the triaxial strains on the Nb<sub>3</sub>Sn in this conductor, and the details are presented in Refs. 9 and 10. The computer code, MAXIMSUPER, treats a single, cylindrical repeating element of the entire multifilament composite. This single superconducting filament or tube represents the average geometry and configuration (niobium-core radius, Nb<sub>3</sub>Sn-layer thickness, bronze-to-niobium ratio, and the amount of copper matrix separating each filament from its nearest neighbors). Since this average filament is repeated in a multifilamentary composite superconductor for thousands of elements, its resulting strain fields from thermal expansion and axial loading should be fairly representative of the overall composite behavior. Of course, this modeling is more accurate for conductors with uniform high filament densities across the composite cross-sectional area. The code determines the three-dimensional strain fields by solving Hooke's elasticity equations for an element composed of the various materials (niobium, Nb<sub>3</sub>Sn, bronze, and copper) in their

representative proportions. The code then iterates the elastic solutions with known plasticity data, such as the stress-strain curves of each material, to obtain an approximate plastic solution. Since the calculated stresses and strains are reported as three-dimensional axial  $\epsilon_z$ , radial  $\epsilon_r$ , and azimuthal  $\epsilon_\theta$  components, we calculate a geometric average strain designated as the effective strain, where  $\nu$  is the Poisson's ratio,

$$\langle \epsilon \rangle = \frac{\sqrt{2}}{2(1+\nu)} \left[ (\epsilon_r - \epsilon_\theta)^2 + (\epsilon_\theta - \epsilon_z)^2 + (\epsilon_z - \epsilon_r)^2 \right]^{1/2} \quad (1)$$

One unique distinction is demonstrated by the MAXIMSUPER strain field predictions for the bronze-core filament geometry as compared to the niobium-core configuration. While the two conductor designs yield approximately the same  $z$  component strains  $\epsilon_z$ , the radial  $\epsilon_r$  and azimuthal  $\epsilon_\theta$  strains are much higher for the bronze-core filament design. To illustrate this effect, we use the geometrical averaging of the three-dimensional strain fields to calculate the effective strain in equation 1 and plot this value against the intrinsic  $\epsilon_z$  strain component for a typical bronze-core and a typical niobium-core filament conductor in Fig. 1. Note that the effective strains are much higher for the

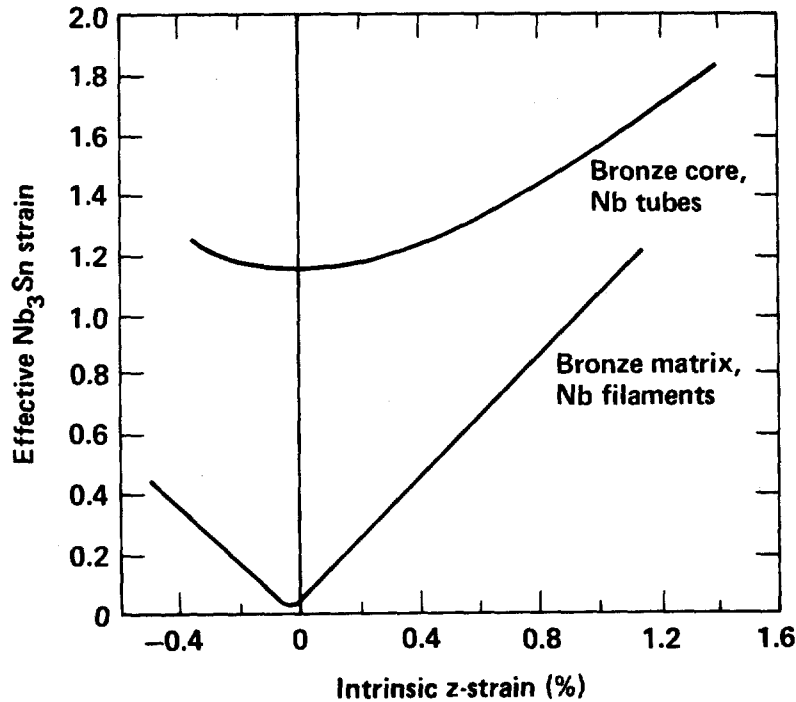


Fig. 1. The effective strain on the Nb<sub>3</sub>Sn layers obtained from Eq. 1 is plotted vs. the intrinsic  $z$  strain for the bronze core-Nb tube and the Nb filament, bronze matrix geometries.

bronze-core sample, because of the contributions from the larger tangential strain components. Other studies have concluded that the peak critical currents occur at approximately zero strain; however, for the bronze-core geometry, the zero intrinsic  $\epsilon_z$  strain values, which give the peak critical current, coincide with nonnegligible tangential strain components on the Nb<sub>3</sub>Sn zones. Hence, the maximum current displayed at zero intrinsic strain is the result of a minimum in the effective average of the three-dimensional strain field, and the minimum value is not necessarily zero. Analytical expressions involving Hooke's elasticity equations in cylindrical geometry show that the mechanical interactions and hence the stress-strain relations are not symmetric with respect to the interchange of the material positions in a fiber composite. In fact, the effective strain increases linearly (Fig. 1) with axial loading for the niobium core and quadratically for the bronze-core geometry. This prediction is experimentally verified in Fig. 2, which is a plot of the measured critical current density of several conductors at  $H = 12$  Tesla and a resistivity ( $\rho_r = 10^{-11} \Omega \cdot \text{cm}$ ) as a function of the MAXIMSUPER predicted residual effective strain (before tensile loading). In general it shows that, for the same bronze-to-Nb<sub>3</sub>Sn ratio, we should expect the bronze-core geometry to be inferior to the

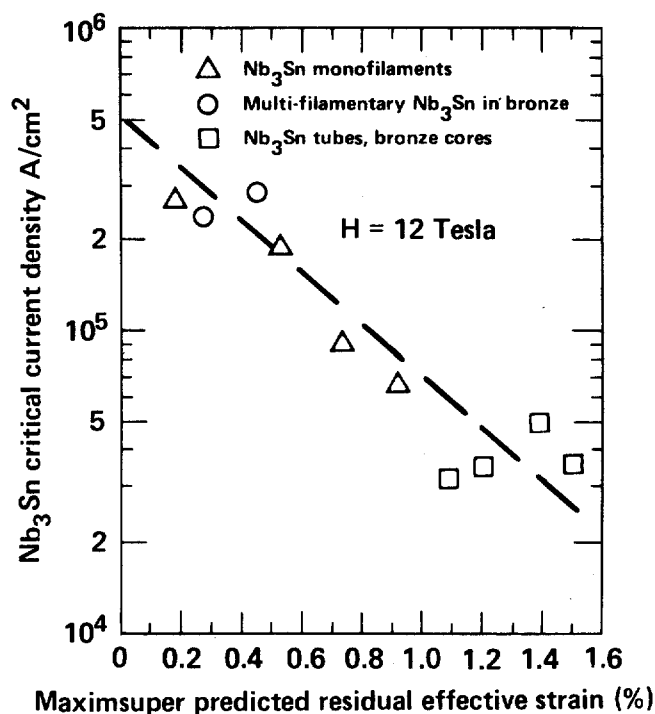


Fig. 2. The measured critical current density as a function of residual strain predicted by the computer code is plotted for various conductor geometries.

Table I. Transition Temperature (K) of Nb<sub>3</sub>Sn Fabricated by the Internal Bronze Approach (Measured Inductively)

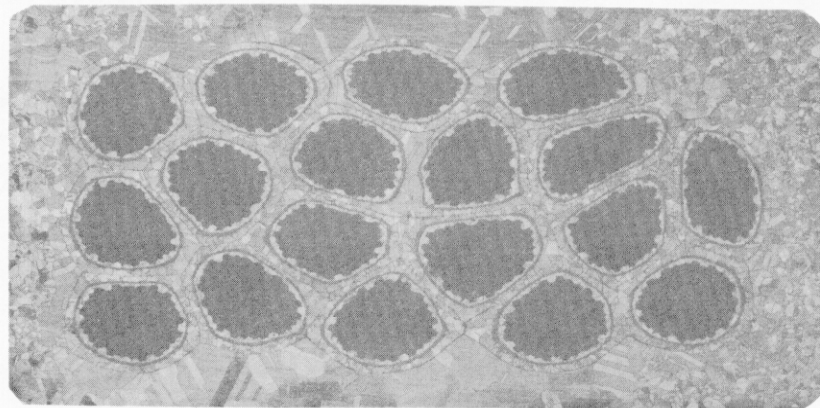
	$T_c$ (Midpoint)	$T_c$ (Onset)
As Fabricated	16.20	17.35
With Cu Matrix Removed	16.50	---
With Bronze Core Removed	17.97	18.10

niobium-core design, with a decrease in critical current density at 12 T of factors from three to ten times.

Some corroborating data on this effect, obtained on these and other internal bronze samples by K. Aihara, T. Luhman, and M. Suenaga,<sup>11,12</sup> are shown in Table 1. For a comparable bronze-to-Nb ratio, the transition temperature depression in the internal bronze conductor is about 1.8 K, compared with about 0.2 K for an external bronze conductor.<sup>12</sup> Similarly, if we plot the transition temperature reduction for the internal bronze sample on a master plot<sup>13</sup> of  $T_c$  reduction versus strain, this plot would indicate a strain of greater than 1 percent in the Nb<sub>3</sub>Sn layer.

#### HFTF Nb<sub>3</sub>Sn SUPERCONDUCTOR

A cryostable Nb<sub>3</sub>Sn conductor designed to operate at 5 kA and 12 T is being manufactured for the High Field Test Facility.<sup>2</sup> This conductor consists of a core which is clad with half-hard Cu after reaction. The core cross-section (Fig. 3) consists of



2 mm

Fig. 3. Cross section of the HFTF conductor core. The core consists of 18 strands in a Cu matrix; each strand contains 15,895 Nb<sub>3</sub>Sn filaments.

58 percent Cu, 30 percent bronze, 10 percent Nb<sub>3</sub>Sn and 2 percent Ta. The Cu in the core is annealed during the reaction step and contributes little to the precompression on the Nb<sub>3</sub>Sn.<sup>11</sup> During the reaction, the bronze is depleted of Sn and is annealed. The resulting precompression of the Nb<sub>3</sub>Sn can be predicted by graphical means and by computer modeling, when the properties of annealed, Sn-depleted bronze are used. In addition, the strain-critical current behavior can be modeled by introducing a strain dependence for the parameters in Kramer's scaling laws.<sup>14</sup> The experimental strain-critical current behavior of the HFTF core is shown in Fig. 4. We also present preliminary bending data for comparison with the tensile strain data. The initial increase in critical current seen in the tensile tests is not evident for the bending tests. However, the tensile data does provide adequate data with which to predict general bending behavior for this conductor.

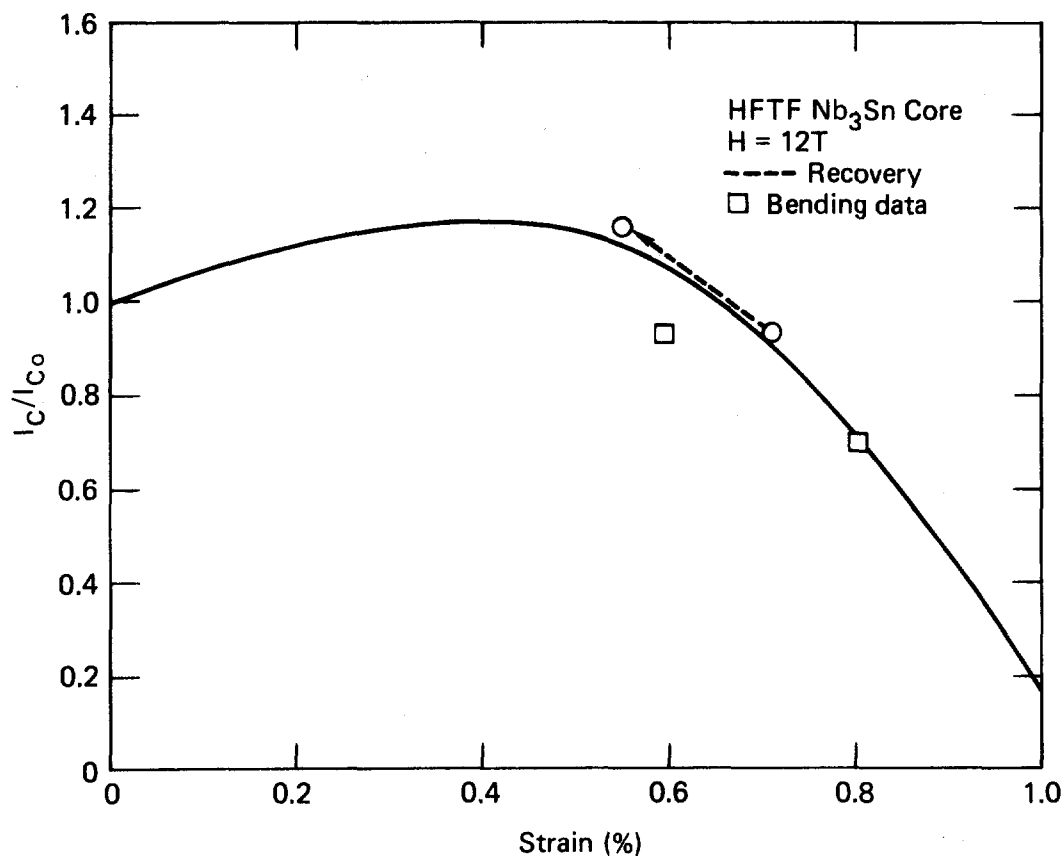


Fig. 4. The critical current (normalized to the value for zero applied strain) is plotted as a function of applied tensile strain for the HFTF core. The change in critical current with applied tensile strain is reversible up to a strain of 0.7 percent.



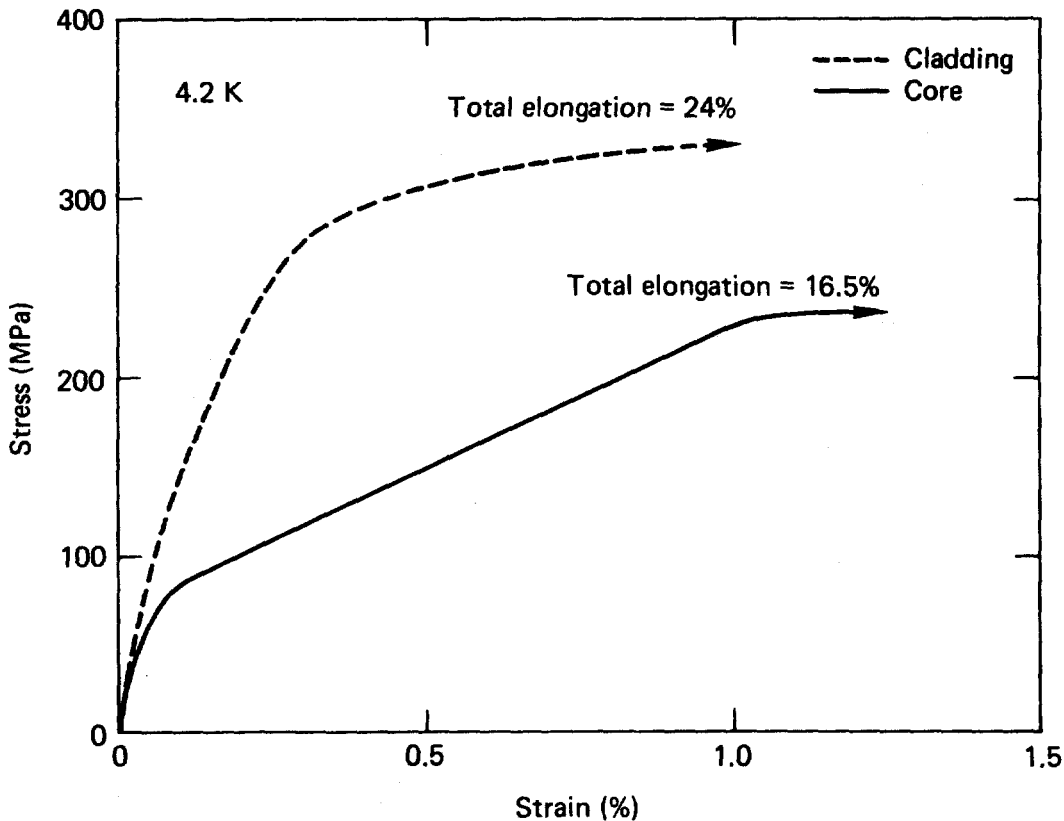


Fig. 5. Experimental stress-strain data for the HFTF core and HFTF cladding at 4.2 K. The cladding is half-hard Cu.

Subsequent to the reaction to form  $\text{Nb}_3\text{Sn}$ , additional Cu (equivalent to approximately 50 percent of the total cross section) is soldered to the core. This Cu has a yield strength of approximately 300 MPa (Fig. 5); hence, it will contribute to the precompression on the  $\text{Nb}_3\text{Sn}$  when the conductor is cooled from the cladding temperature to the 4.2 K operating temperature. The calculated value of additional precompression on the  $\text{Nb}_3\text{Sn}$  due to differential thermal contraction between 553 K and 4.2 K is 0.5 percent. This precompression occurs in two steps: during the cooling from cladding temperature to 293 K and during cooling from 293 K to 4.2 K. The amount of compressive strain actually transmitted to the  $\text{Nb}_3\text{Sn}$  during the first step depends upon the experimental conditions, in particular, the extent that the solder between core and cladding yields during the cladding operation. Experiments are in progress to measure the additional precompression in the HFTF conductor due to the Cu cladding.

This precompression, due to the cladding, is useful from the standpoint of providing more strain tolerance during coil winding

and coil operation. However, the Nb<sub>3</sub>Sn critical current is reduced due to the compression; this must be taken into account in designing the conductor.

Additional precompression can be expected for the JAERI design of the TMC conductor<sup>15</sup> and other designs employing cold-worked copper for stabilization.

#### LCP-TYPE CONDUCTOR

Another Nb<sub>3</sub>Sn-base conductor of practical interest is the forced-flow conductor being utilized in the LCP.<sup>1</sup> Strands of 0.7-mm diameter multifilamentary Nb-bronze are insulated, cabled, and wrapped in a stainless steel jacket prior to heat treatment to form Nb<sub>3</sub>Sn. The strain-critical current behavior of the individual strands has been measured<sup>16</sup> and the results are adequately predicted by the analytical method.<sup>7</sup> In order to verify the behavior of these strands in the final conductor, a series of samples were prepared<sup>17</sup> for testing in the LLNL tensile testing facility. The samples consisted of 81-strand cables which were compacted in type 304 stainless steel tubes, with approximately 33 percent of the cross sectional area available for helium coolant (Fig. 6). The ends of the sample were compacted, to form current terminations, and pinned to the steel jacket, to insure that the strain was imparted to both the cable and the jacket. Strain gages and voltage taps were placed on the samples in the 5-cm uniform field zone of the test magnet. The strain-critical current behavior for these samples is illustrated in Fig. 7 and compared with the single-strand data. The initial critical current values (for H = 8 T) are suppressed to 75 percent of the single-strand values, and the peak in critical current is shifted from ~0.2 percent applied strain to ~0.8 percent applied strain. Although the strain-critical current behavior for the single strands and the total conductor are quite different, the critical current value at the peaks is the same for the two cases. In order to verify that this behavior is due to the stainless steel jacket, identical samples with soft copper jackets were tested (Fig. 7). These critical current values scaled directly to the values for the single strands.

The behavior of the jacketed conductor compared with that for the single strands becomes evident when the thermal contraction of the stainless steel jacket is considered. The stainless steel jacket comprises about 47 percent of the conductor cross section and has a mean thermal expansion coefficient  $\alpha = 15.3 \times 10^{-6}/^{\circ}\text{K}$ . The temperature range over which the differential thermal contraction of the stainless steel must be considered is from the reaction temperature (973 K) to 4.2 K. When the properties of the stainless steel are considered, two factors become important: (1) the dif-

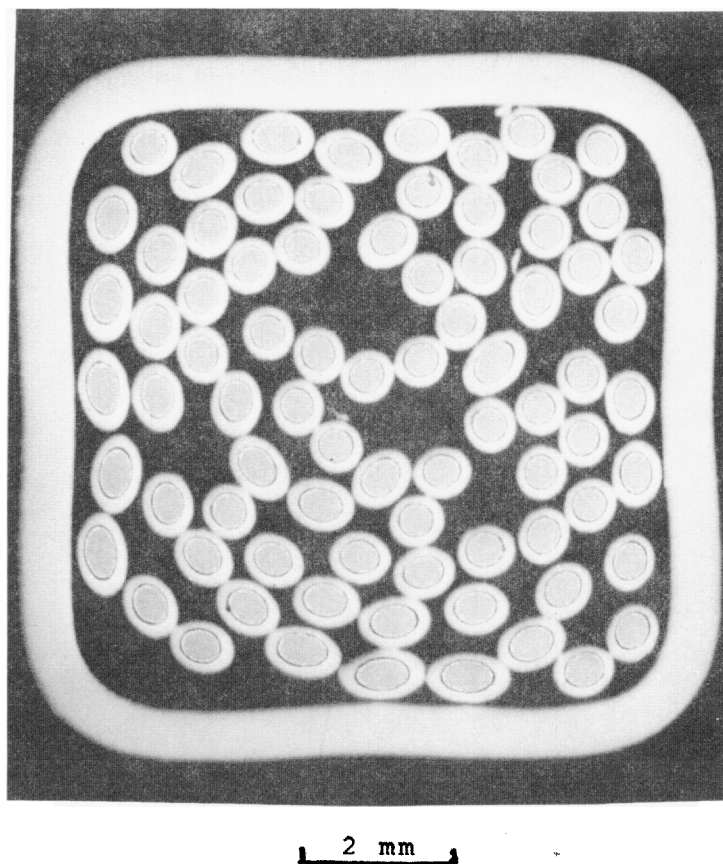


Fig. 6. Cross section of the LCP-type conductor used in the strain-critical current experiments.

ferences in thermal expansion coefficients (stainless steel to  $\text{Nb}_3\text{Sn}$  and bronze to  $\text{Nb}_3\text{Sn}$ ) are similar; (2) the higher yield stress of the stainless steel compared to that of bronze, especially at higher temperatures, means that the stainless steel is much more effective in applying a compressive strain to the  $\text{Nb}_3\text{Sn}$ . When the data appropriate for stainless steel are used to calculate the precompression on the  $\text{Nb}_3\text{Sn}$ , a value of 0.8 percent precompressive strain is obtained, in good agreement with the experimental results shown in Fig. 7. This value of precompression is greater than that necessary to protect the  $\text{Nb}_3\text{Sn}$  from damage during winding and operation. Moreover, the decrease in critical current at 12 T, compared to the unstrained case, is a factor of two. Consequently, this configuration presents a significant design problem to be overcome if the operation at 12 T is to be optimized.

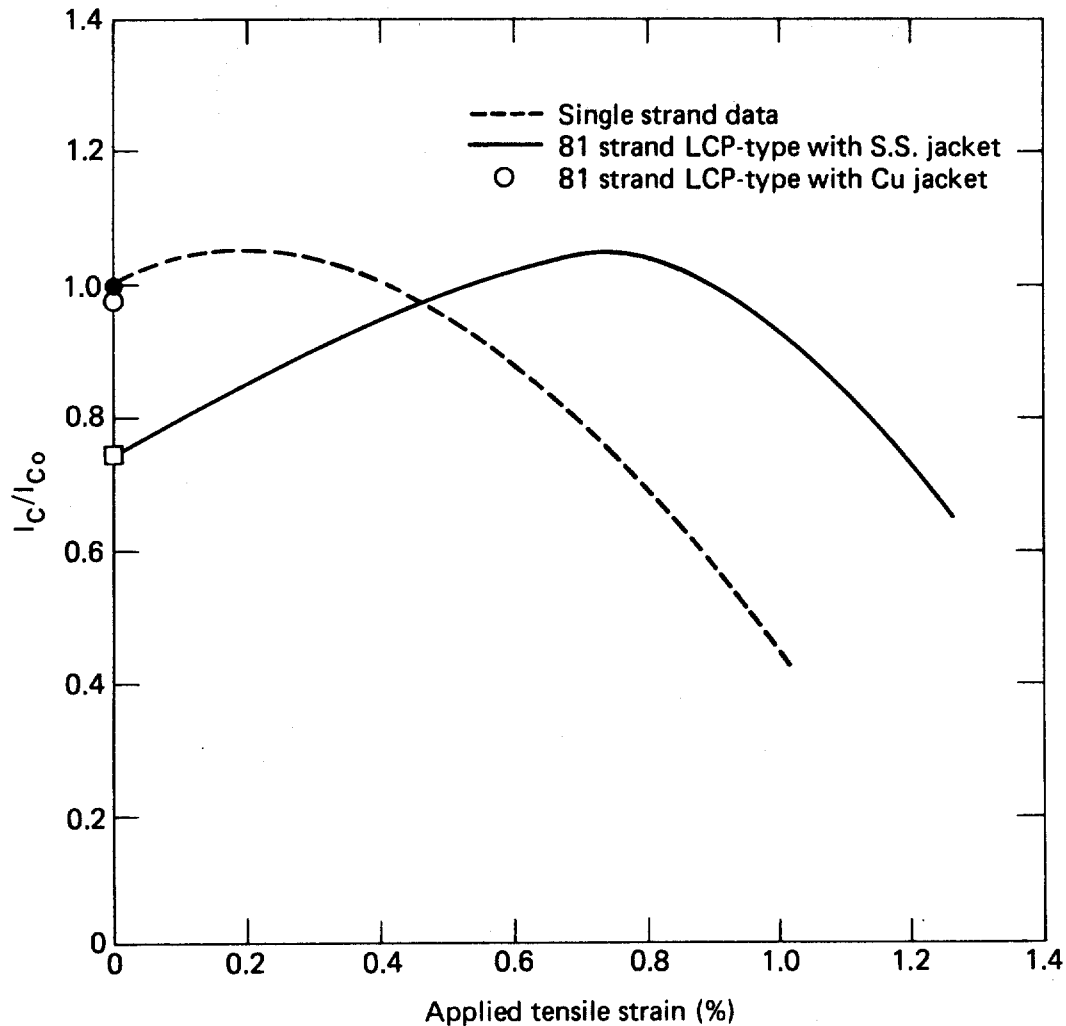


Fig. 7. The critical current (normalized to the value for zero applied strain on a single strand) is plotted as a function of applied tensile strain for a single strand and for 81-strand LCP-type conductors.

#### CONCLUSIONS

The behavior expected for several configurations of  $Nb_3Sn$  conductors has been calculated and measured. The results show that the triaxial strain state of the  $Nb_3Sn$  is important for understanding the behavior of the Nb tube, bronze-core geometry.

For practical conductors in which stainless steel or work-hardened Cu are used to provide strength, the additional

precompression on the Nb<sub>3</sub>Sn due to these components must be taken into account.

#### ACKNOWLEDGMENTS

The preparation of the LCP-type samples by P. Sanger and co-workers at Airco Superconductors is gratefully acknowledged. The bronze-core, Nb-tube samples were manufactured by Supercon, Inc. Experimental assistance in sample measurements was provided by D. Hirzel, J. Johnston, and P. Waide at LLNL.

#### REFERENCES

1. P. A. Sanger, E. Adam, E. Gregory, W. Marancik, E. Mayer, G. Rothschild, and M. Young, IEEE Trans. on Magnetism, MAG-15, 789 (1979).
2. D. N. Cornish, H. L. Harrison, A. M. Jewell, R. L. Leber, A. R. Rosdahl, R. M. Scanlan, and J. P. Zbasnik, "Progress on Lawrence Livermore Laboratory's Superconducting High-Field Test Facility," in Proc. 8th Symp. on Eng. Problems of Fusion Research, San Francisco, CA (1980).
3. M. S. Walker, J. M. Cutro, B. A. Zeitlin, G. M. Ozeranski, R. E. Schwall, C. E. Oberly, J. C. Ho, and J. A. Woollam, IEEE Trans. on Magnetism MAG-15, 80 (1979).
4. Many articles on the effects of strain on critical properties of Nb<sub>3</sub>Sn are found in the Proc. of the 1976 and 1978 Appl. Supercon. Conf. (IEEE Trans. on Magnetism MAG-13 and MAG-15) and in Adv. in Cryogenic Engineering 24 (1978).
5. T. Luhman, M. Suenaga, and C. J. Klamut, Adv. in Cryogenic Engineering 24, 325 (1978).
6. G. Rupp, Cryogenics 18, 663 (1978).
7. D. S. Easton, D. M. Kroeger, W. Specking, and C. C. Koch, to be published in J. Appl. Physics.
8. R. M. Scanlan, D. N. Cornish, J. P. Zbasnik, R. W. Hoard, J. Wong, and R. Randall, to be published in Adv. in Cryogenic Engineering 26.
9. R. W. Hoard, R. M. Scanlan, and D. G. Hirzel, *ibid.*
10. R. W. Hoard, Ph.D. Thesis, Univ. of Washington, to be published.
11. K. Aihara, M. Suenaga, and T. Luhman, in Proc. 8th Symp. on Eng. Problems of Fusion Research, San Francisco, CA (1980).
12. M. Suenaga, private communication.
13. D. O. Welch, Adv. in Cryogenic Engineering 26, to be published.
14. E. Kramer, J. Appl. Phys. 44, 1360 (1973).
15. S. Shimamoto, T. Ando, H. Tsuji, M. Nishi, E. Tada, K. Yoshida, and K. Yasukochi, in Proc. 8th Symp. on Eng. Problems of Fusion Research, San Francisco, CA (1980).

16. W. Specking, D. S. Easton, D. M. Kroeger, and P. A. Sanger, Adv. in Cryogenic Engineering 26, to be published.
17. Samples were prepared by P. Sanger, AIRCO Superconductors.

#### NOTICE

Reference to a company or product name does not imply approval or recommendation of the product by the University of California or the U.S. Department of Energy to the exclusion of others that may be suitable.

"This report was prepared as an account of work sponsored by the United States Government. Neither the United States nor the United States Department of Energy, nor any of their employees, nor any of their contractors, subcontractors, or their employees, makes any warranty, express or implied, or assumes any legal liability or responsibility for the accuracy, completeness or usefulness of any information, apparatus, product or process disclosed, or represents that its use would not infringe privately-owned rights."